EXPERIMENTAL INVESTIGATIONS ON THE LATERAL BEARING BEHAVIOR OF VIBRATORY-DRIVEN OPEN STEEL PIPE PILES

Johannes Labenski, Institute for Geotechnical Engineering (IGS), University of Stuttgart, Germany, PH: +49 711 685 63779; email: johannes.labenski@igs.uni-stuttgart.de

Christian Moormann, Institute for Geotechnical Engineering (IGS), University of Stuttgart, Germany, email: christian.moormann@igs.uni-stuttgart.de

ABSTRACT

The paper describes the experimental setup used at the Institute for Geotechnical Engineering (IGS) at the University of Stuttgart to investigate the lateral load bearing behaviour of vibratory-driven steel pipe piles in dense saturated sand. The test material, the measurement devices and the experimental procedure are explained in a comprehensive manner. Afterwards the result of the pile installation and the lateral load test of one representative model test are shown and explained for one typical test in detail. The results are given in dimensionless values, i.e. a comparison with other model tests documented in literature is possible. To demonstrate the installation behaviour, the pile penetration velocity and the vertical acceleration measured at the pile head are shown. The lateral load bearing behaviour is investigated using a lateral load-displacement curve of the pile head. The experimental lateral load-displacement curve is compared with analytically determined curves using different p-y approaches. This comparison shows partially good agreement between model test and analytical solution. Nevertheless, it indicates need for further investigation, which is an ongoing process at the IGS.

Keywords: vibratory driving, steel pipe piles, monopile, lateral bearing behaviour, soil-pile-interaction

INTRODRUCTION

The lateral load bearing behaviour of open steel pipe piles depends, among others, on the pile diameter, the embedment length of the pile, the interface friction angle between the pile and the soil, the relative density of the soil and the installation method. During the vibratory-driven installation the pile is vertically excited by a dynamical force acting down- and upwards. This vertical excitation of the pile leads to an excitation of the soil grains which are moved not only vertically, but also horizontally (Hartung 1994). In accordance with findings by Hartung (1994) for piles vibratory driven with a frequency of 40 - 50 Hz, the soil around the pile shaft during installation can be divided into two different zones: a liquefaction zone close to the pile shaft and a compaction zone. Due to the dynamical excitation the soil grains in the liquefaction zone are moving with high velocities leading to a higher volume of the soil in this area. After pile driving, the relative density in the liquefaction zone is low while there is a high relative density in the compaction zone. In the area around the pile toe, the soil is behaving similarly.

Current research by e.g. Kallehave et al. (2012) or Klinkvort et al. (2013) on the lateral load bearing behaviour of monopiles focuses on the modification of current approaches, e.g. the p-y approach (DNVGL-ST-0126). In this research pile installation effects are neglected, while the influence of different lateral load situations is investigated. In literature only one large scale field test is documented investigating the lateral load bearing behaviour of vibratory-driven monopiles (cf. Moormann et al. 2016). In this field test, a slightly stiffer lateral load bearing behaviour has been observed, if the pile was impact-driven. This lack of research was motivation to conduct own experimental tests with the focus on the investigation of the influence of installation effects due to vibratory pile driving on the lateral load bearing behaviour.

EXPERIMENTAL SETUP

Test Material – Sand

The scaled model tests have been conducted with saturated Berlin Sand. The corresponding grain size distribution curve is shown in Fig. 1. The sand has a maximum density $\rho_{d,max}$ of 1.856 g/cm^3 corresponding to a minimum void ratio of 0.433, as well as a minimum density $\rho_{d,min}$ of 1.563 g/cm^3 corresponding to a maximum void ratio of 0.702. Further laboratory tests on the sand used for the tests are provided by Le (2015).

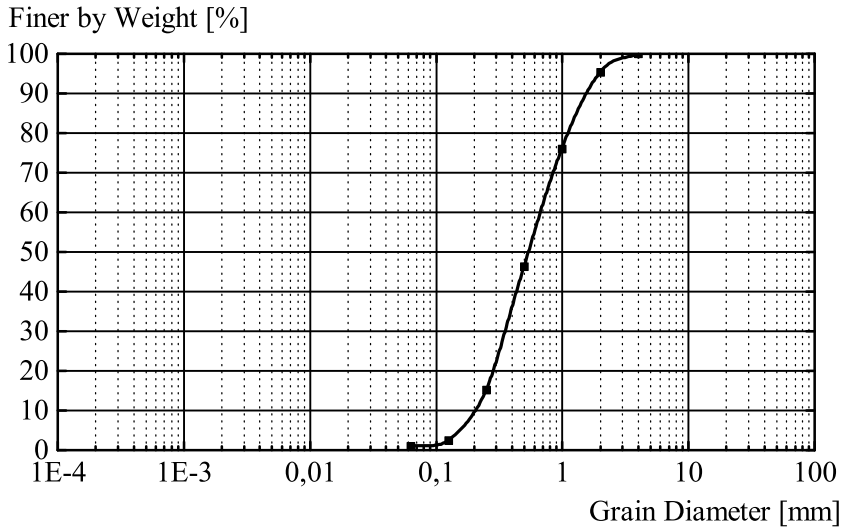

Fig. 1. Grain size distribution curve of Berlin Sand used in the scaled model tests

Test Material – Pile

The properties of the model pile are depicted in Table 1. In reality steel tube piles are used as monopiles. In the scaled model tests, a glass-fibre reinforced pile has been used instead to accurately scale down the flexural rigidity of the pile (cf. Wood 2004). A picture of the pile is shown in Fig. 2. The dimensions of the pile lead to an L/D ratio of 4.2, which is typical for monopiles.

Table 1. Properties of the model pile

Property	Unit	Value
Diameter	[m]	0.208
Length	[m]	2.00
Embedment length	[m]	0.87
Wall thickness	[m]	0.0032
Mass	[kg]	10.0
Mass incl. vibrator and vibrator mount	[kg]	75.0
Flexural rigidity EI	[kNm^2]	550

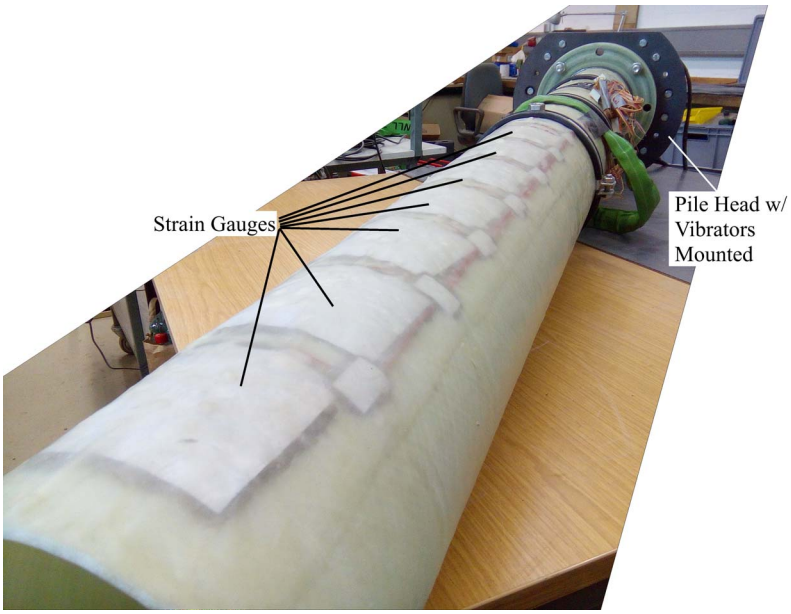

Fig. 2. Photo of the model pile

Test Container and Measurement Devices

The set-up of the 1-g model scaled tests is illustrated in Fig. 3. The scaled model tests were conducted in a cylinder shaped concrete container with a diameter of 2.0 m and a height of 2.5 m. The container was filled with a 0.3 m drainage layer followed by 2.2 m of Berlin Sand. The two layers were separated by a fleece. The whole concrete container can be flooded with water rising from the bottom, which has the advantage that the structure of the installed sand is not disturbed and remained homogeneous while being saturated (cf. Tasan 2011). The dimensions of the concrete container ensure a horizontal distance of 4.5D from the external pile shaft surface to the boundaries and a vertical distance of 7.5D from the bottom of the pile to the bottom of the concrete container.

During the pile installation, the acceleration at the pile head was measured with a triaxial accelerometer. Furthermore, a position transducer was continuously monitoring the penetration of the pile. In further tests, acceleration sensors have been placed within the soil to precisely investigate the dynamic behaviour of the sand during pile installation. During the horizontal pile load test, the bending moment of the pile was measured with strain gauges, which were placed along the part of the pile shaft that is embedded into the sand. Only one pair of strain gauges was placed at the pile head where no bending occurs, i.e. temperature effects can be compensated. In total, nine strain gauge measurement layers were placed on the pile. Furthermore, the pile head displacement was measured with three displacement sensors. With these two quantities, the bending curve of the pile could be back-calculated. Also the horizontal force was continuously monitored and recorded during the horizontal pile load test. In Table 2 the abbreviations used in Fig. 3 are documented.

Table 2. Sensors used in the scaled model test

Sensor	Shortcut
Acceleration Sensor	ACC
Position Transducer	PT
Strain Gauges	DMS 1..9
Load Cell	H_0
Displacement Transducer	W1, W2, W3

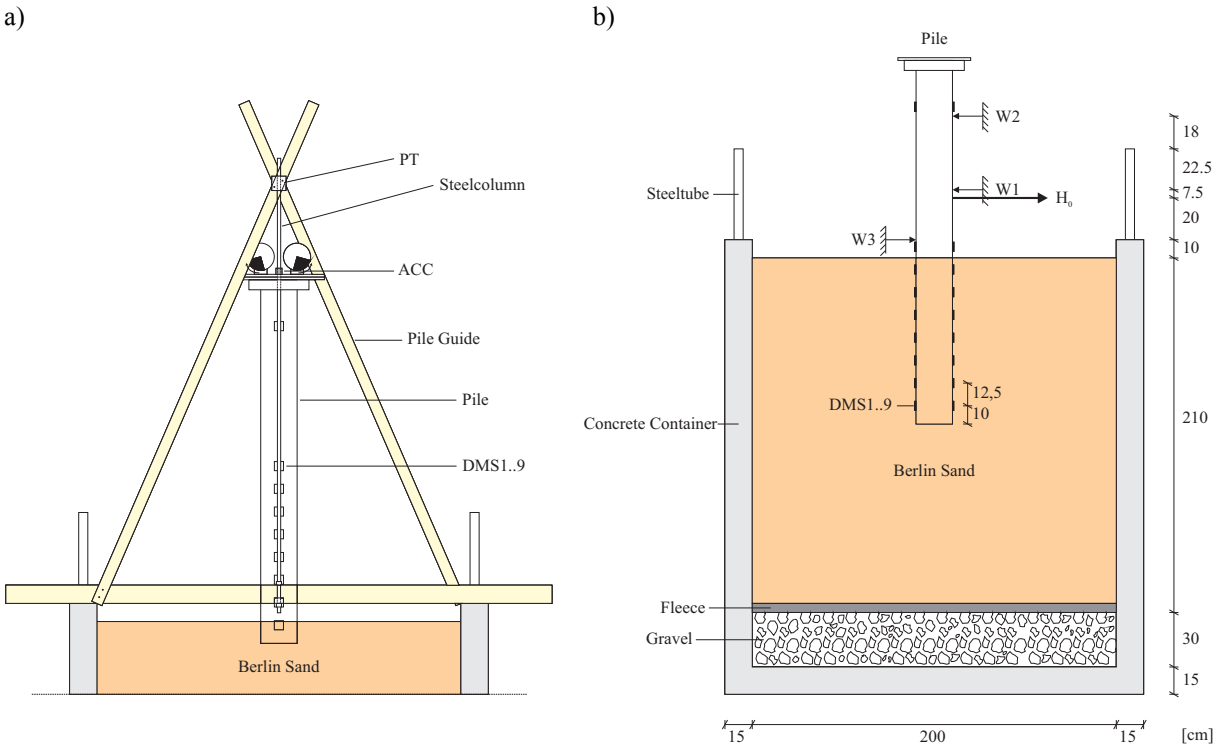

Fig. 3. Model setup a) for pile installation and b) for lateral pile load test

Experimental Procedure

The main target of the scaled model tests was to investigate the influence of different installation parameters on the lateral load bearing behaviour of vibratory-driven monopiles. Installation parameters are the frequency f and the static moment M_{stat} of the vibrators. Besides the installation parameters, also the density of the sand was varied. The scaled model tests were carried out under 1g conditions.

The scaled model tests consist of different steps. In the first step, the sand was filled homogeneously in the model container. In the second step, the pile was vibratory-driven to the desired embedment depth. In the third step, a lateral pile load test was carried out to investigate the lateral load bearing behaviour.

The tests were conducted in medium-dense, dense and very-dense sand. The sand was installed layer by layer. Trickling of the sand was not possible, because the sand could not be dried after each test, thereby remaining moist. Every layer was compacted by an electrical vibratory plate.

The pile was installed in the sand with a vibrator unit generating a maximum centrifugal force of 4.4 kN at a frequency of 25 Hz. Two WUERGES HV 6/4-18 were mounted on top of the pile via two steel plates. The frequency and harmony of the vibrators was controlled by a frequency converter.

The lateral pile load test was carried out with a pneumatic cylinder, which generates the tension force H_0. The pneumatic cylinder can be controlled by an electric function generator. This setup has the advantage that only with slight modifications a cyclic lateral force can be applied as well.

Prior to the test series with the vibratory-driven piles, a reference test was carried out by jacking a pipe pile instead of vibrating. A maximum force of 25 kN was needed to push the pile to the desired embedment depth, which exceeds the maximum centrifugal force of the vibrator by a factor of 5.5.

SELECTED RESULTS

Pile Installation

In the following section results of a representative model test are shown. Different dimensionless values are introduced to investigate the results.

The installation parameters can be expressed as a dimensionless frequency f^* and a dimensionless static moment M_s^*:

$$f^* = \frac{f_{Vibration}}{f_{Resonance}} \quad [1]$$

where $f_{Vibration}$ is the vibration frequency and $f_{Resonance}$ is the investigated resonance frequency of the vibrator-pile-soil system (cf. Massarsch et al. 2017).

$$M_s^* = \frac{M_{stat}}{M \cdot D} \quad [2]$$

where M_{stat} is the static moment of the vibrator, M is the mass of the vibrator-pile system and D is the diameter of the pile.

As depth, the relative embedment depth L^* is introduced, which is defined as follows:

$$L^* = \frac{L(t)}{L_{Vibration}} \quad [3]$$

where $L(t)$ is the measured vibration depth at time t and $L_{Vibration}$ is the total length installed by vibration.

In the presented model test the pile was vibratory driven with a $f^* = 0.82$ and a $M_s^* = 0.0075$ in dense sand. In Fig. 4 the penetration velocity over depth as well as the vertical acceleration measured at the pile head over installation time are shown. Positive accelerations are directed downwards in penetration direction. Negative accelerations are directed upwards, against penetration direction.

The velocity profile presented in Fig. 4a shows a decrease of velocity with increasing embedment depth. At the start of the installation process the penetration velocity has its maximum at 55 mm/s and already drops to 30 mm/s after 10% of pile penetration. Afterwards it is increasing and decreasing again in a pseudo sinusoidal pattern. This may be due to minor inhomogeneities during the sand preparation process. Nevertheless, in these two regions, a mean velocity can be considered. It can be noted, that these regions have the same size, i.e. $\Delta L^* = 0.3$ for both regions. In the first region between $L^* = 0.1$ and $L^* = 0.4$ a mean velocity of 25 mm/s can be considered. In the next region between $L^* = 0.4$ and $L^* = 0.7$ the mean velocity decreases to 20 mm/s. Between $L^* = 0.7$ and $L^* = 1.0$ the penetration velocity decreases drastically to a value of 2.5 mm/s just before the end of the penetration process. The large decrease of penetration velocity at the beginning of the installations emerges from the small initial embedment depth of the pile. At the beginning of the installation process, the pile can more or less move free. After 10 % of pile penetration, it is likely that the soil resistance at the pile toe and shaft increases and the penetration velocity decreases.

Pile penetration is only possible, if there are plastic deformations in the surrounding soil. If there were only elastic deformations, no (further) pile penetration could be possible. Between $L^* = 0.7$ and $L^* = 1.0$ it seems that the soil behaviour around the pile is transforming from a plastic behaviour to an elasto-plastic or almost elastic behaviour. This effect might result from a densification of the

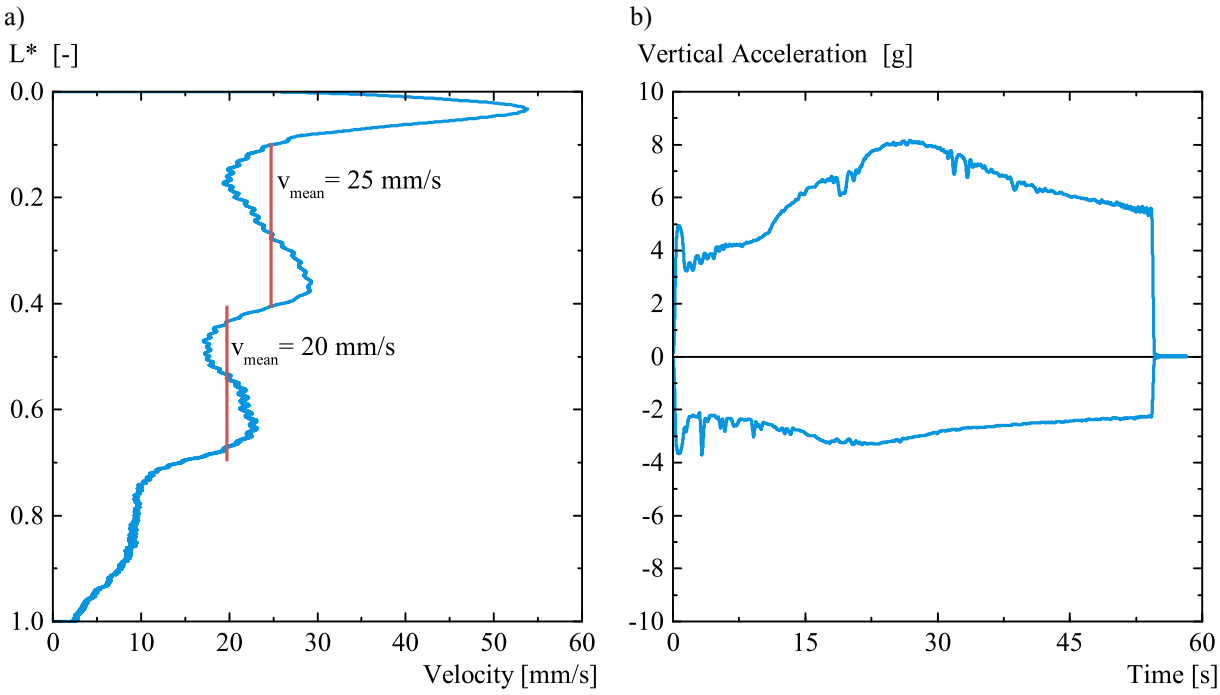

Fig. 4. a) Pile penetration velocity over relative embedment depth; b) Vertical acceleration measured at the pile head during installation

surrounding sand. If the sand is densified, the shaft resistance of the pile increases. With an increased shaft resistance, the displacement amplitude of the pile reduces and thus, also the penetration velocity.

Another possible reason might be arching of the soil within the pile and thus a higher soil resistance. This reason is supported by observations during the model test. After completion of the test, as the pile was extracted from the sand, a soil plug inside the pile was extracted too. This might be a "local" effect due to the small pile diameter in the scaled model tests, though numerical simulations on vibratory-driven piles revealed an increase of lateral stress acting on the pile shaft at the inside of the pile (cf. Labenski et al. 2016).

The acceleration profile in Fig. 4b shows a strong increase of accelerations directed downwards until a peak value of 8g is reached. After this peak value, the acceleration is decreasing. This decrease corresponds to a depth between $L^* = 0.7$ and $L^* = 1.0$, i.e. when the velocity decreases, the acceleration decreases as well. The vertical acceleration can be directly linked to the displacement amplitude of the pile, i.e. when the displacement amplitude of the pile reduces the pile penetration rate reduces as well for the reasons stated above.

Lateral Pile Load Test

In Fig. 5 the normalised lateral load-displacement curves of the model tests are shown. The horizontal force H_0 was made dimensionless according to Klinkvort et al. (2013) as follows:

$$P^* = \frac{H}{\gamma' D^3 K_p} \quad [4]$$

with

$$K_p = \tan^2(45° + 0.5\,\varphi') \quad [5]$$

$$\varphi' = 31.5° \exp\left(0.42\, I_D^{2.9}\right) \quad [6]$$

according to Le (2015) for Berlin Sand.

The lateral deflection y was made dimensionless as follows:

$$y^* = \frac{y}{D} \quad [7]$$

In the diagram the lateral load scheme can be depicted. The lateral load was increased step-wise. At different load levels, the load was decreased and increased again. The maximum lateral load applied in the model test is considered to be higher than the maximum load in reality..

It can be seen, that the lateral deformations of the vibratory-driven pile are smaller than of the jacked pile. In the mean, the lateral displacements of the jacked pile are increased by a factor of 1.75 in comparison to the vibratory-driven pile.

The load-displacement curve shown in Fig. 5 indicates, creep effects becoming more severe with increased lateral load, especially in the case of the jacked pile. These creep effects may result from a pre-failure stage in the soil. In some tests failure of the soil could be observed as a failure surface developed in the soil on the passive side of the pile.

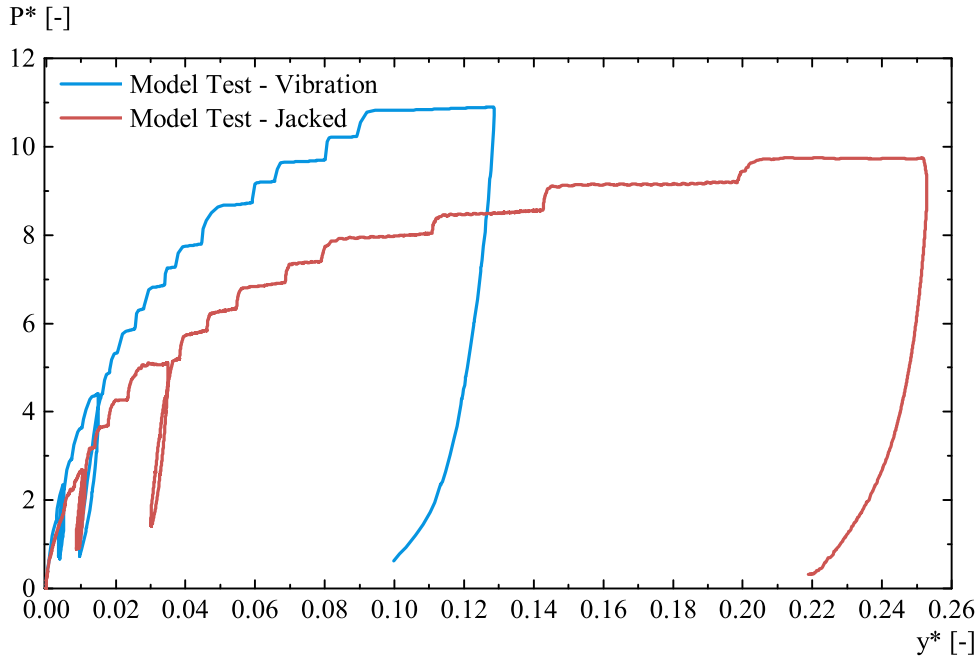

Fig. 5. Normalised lateral load-displacement diagram

COMPARISON

To evaluate the lateral load-displacement curves obtained in the scaled model tests, they are compared with analytical determined lateral load-displacement curves. The p-y approach (cf. DNVGL-ST-0126) was utilized to determine lateral soil reaction springs. In the literature different approaches exist to determine the non-linear spring stiffness in order to take different mechanical and geometrical boundary conditions into account.

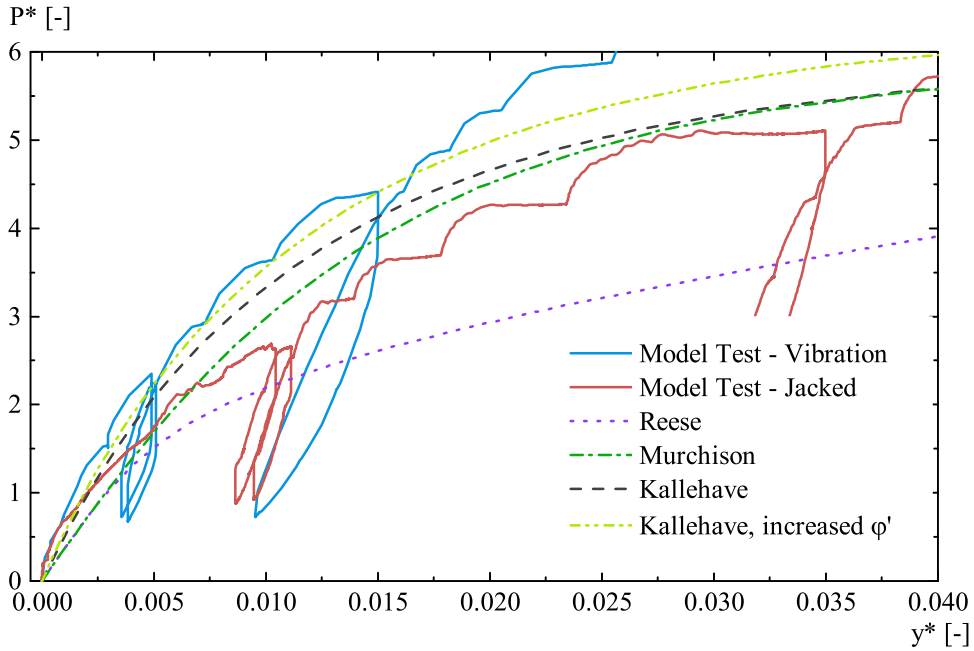

Fig. 6. Normalised lateral load-displacement diagram comparing the result of the scaled model test with the result of the analytical p-y approach

In this paper, the following p-y approaches have been utilized:

- Reese et al. (1974)
- Murchison & O'Neil (1984)
- Kallehave et al. (2012)

The results are presented in Fig. 6. Utilizing the approach by Reese et al. (1974) leads to an overestimation of the true lateral displacements of the vibratory-driven and the jacked pile. This could be expected, as the approach by Reese et al. was originally developed for long slender piles and not for short rigid piles, which are used in the scaled model tests. The approach by Murchison & O'Neil (1984), which is equivalent to the method proposed in DNVGL-ST-0126, shows results closer to the experimental curves. Though this approach is also not validated for monopiles, the characteristics of the load-displacement curve are similar to the experimental curves corresponding to a short rigid pile. This approach overestimates the lateral displacements of the vibratory-driven pile by 30% to 50% in the range of P* = 0 to 5, but underestimates the displacements of the jacked pile only slightly. Considering the modified p-y approach as proposed by Kallehave et al. (2012), even better results can be achieved. The approach by Kallehave et al. (2012) considers an increased soil stiffness at low strain in comparison to the approach by e.g. Murchison & O'Neil (1984). This can be seen in Fig. 6 as well. The initial slope of the experimental load-displacement curve is steeper in comparison to the load-displacement curve obtained with the approach by Murchison & O'Neil (1984), while the ultimate load remains the same. The lateral loading behaviour determined with the modified p-y approach by Kallehave et al. (2012) shows good agreement with the behaviour obtained in the experimental test with the vibratory-driven pile, especially concerning the curvature and slope of the curve up to a lateral load of P* = 4.5.

The comparison of the experimental results with the three analytical determined lateral load-displacement curves shows that with a current modification of the p-y approach suitable for short rigid piles, good agreement can be achieved to the load-displacement behaviour of a vibratory-driven pile in a conservative manner. All presented methods slightly overestimated the lateral displacements. The reason might be the p-y approach itself, as it was not developed for vibratory-driven piles and also current modifications of the p-y approach do not especially consider pile installation effects. As a first

workaround it seems likely to increase the stiffness of the soil springs to achieve better agreement between experiment and analytical solution. This approach was applied, i.e. the friction angle φ' was slightly increased, and is denoted as *Kallehave, increased φ'* in Fig. 6. Very good agreement between the experimental and analytical results can be achieved for the vibratory-driven pile up to a lateral load of P* = 4.5. Even though this approach is only a workaround, it still reveals that due to vibratory-driving lateral load bearing behaviour might become stiffer than analytically determined.

It should be noted, that the ultimate load determined with all the analytical approaches has a value of P* = 6 which is only half of the lateral load applied in the experiment.

CONCLUSIONS

In this paper the experimental setup as well as one representative result of scaled model tests with vibratory-driven piles carried out for 1g conditions has been presented in comparison to the result of a jacked pile. The penetration velocity and the pile head accelerations measured during vibratory-driving have shown that if the pile displacement amplitude reduces, also the penetration velocity reduces. A possible reason might be the densification of the surrounding soil as well as the soil inside of the pile. The comparison of the experimental load-displacement curves of the vibratory-driven pile with the jacked pile has revealed a stiffer lateral load bearing behaviour in case of the vibratory-driven pile. The further comparison of the experimental lateral load-displacement curves with the analytical determined curves has revealed, that with current p-y approaches the lateral load bearing behaviour of short rigid piles can be predicted within a certain range of uncertainty. In the case of a jacked pile, lateral deformations are underestimated whereas in the case of the vibratory-driven pile, lateral deformations are overestimated. The comparison further revealed that the influence of vibratory-driving of monopiles might result in a stiffer lateral load-bearing behaviour than predicted by analytical models. Though, this aspect needs further research and investigation of the test results. Especially the influence of the installation parameters 'frequency' and 'static moment' will be further investigated.

ACKNOWLEDGEMENTS

The tests presented in this paper have been conducted in the frame of the "VibroPile II" project. The authors would like to acknowledge the founding by innogy SE and the support of Ben Matlock and Volker Herwig. The calculations presented in this publication were performed with the IGtHPile software developed by the Institute of Geotechnical Engineering (IGtH), Leibnitz Universität Hannover, Germany.

REFERENCES

DNVGL-ST-0126, April 2016: Support structures for wind turbines. DNV GL Standard.

Hartung, M, 1994: Einflüsse der Herstellung auf die Pfahltragfähigkeit in Sand. Dissertation, Institut für Grundbau und Bodenmechanik, Technische Universität Braunschweig, Heft 45.

Kallehave, D., LeBlanc, C., and Liingaard, M.A., 2012: Modification of the API p-y formulation of initial stiffness of sand. Offshore Site Investigation and Geotechnics: Integrated Technologies - Present and Future, 12-14 September. Society of Underwater Technology, London. pp. 465–472.

Klinkvort, R.T., Hededal, O., and Springman, S., 2013: Centrifuge modelling of drained lateral pile - soil response: Application for offshore wind turbine support structures. Dissertation, Technical University of Denmark.

Labenski, J., Moormann, C., Aschrafi, J., and Bienen, B., 2016: Simulation of the plug inside open steel pipe piles with regards to different installation methods. Proceedings of the 13th Baltic Sea Geotechnical Conference. Vilnius Gediminas Technical University, Vilnius, Lithuania. pp. 223–230.

Le, V.H., 2015: Zum Verhalten von Sand unter zyklischer Beanspruchung mit Polarisationswechsel im Einfachscherversuch. Dissertation, Fachgebiet Grundbau und Bodenmechanik, Technische Universität Berlin, Heft 66.

Massarsch, K.R., Fellenius, B.H., and Bodare, A., 2017: Fundamentals of the vibratory driving of piles and sheet piles. geotechnik, 40(2): 126–141.

Moormann, C., Kirsch, F., and Herwig, V., 2016: Vergleich des axialen und lateralen Tragverhaltens von vibrierten und gerammten Stahlrohrpfählen. Proceedings of the 34. Baugrundtagung, DGGT. Bielefeld. pp. 73–81.

Murchison, J.M., and O'Neill, M.W., 1984: Evaluation of p-y relationships in cohesionless soils. Proceedings of the ASCE Symposium Analysis and Design of Pile Foundations, 01-05 October, San Francisco. pp. 174–191.

Reese, L.C., Cox, W.R., and Koop, F.D., 1974: Analysis of laterally loaded piles in sand. Offshore Technology Conference, 1974, Houston, Texas.

Tasan, E., 2011: Zur Dimensionierung der Monopile-Gründungen von Offshore-Windenergieanlagen. Dissertation, Fachgebiet Grundbau und Bodenmechanik, Technische Universität Berlin, Heft 52.

Wood, D.M., 2004: Geotechnical modelling. E. & F.N. Spon.